Bone mesenchymal stem cells pretreated with erythropoietin accelerate the repair of acute kidney injury

song zhou
Zhujiang Hospital
Yu-ming Qiao
Zhujiang Hospital
Yong-guang Liu
Zhujiang Hospital
Ding Liu
Zhujiang Hospital
Jian-min Hu
Zhujiang Hospital
Jun Liao
Zhujiang Hospital
Min Li
Zhujiang Hospital
Ying Guo
Zhujiang Hospital
Li-pei Fan
Zhujiang Hospital
Liu-Yang Li
Zhujiang Hospital
Ming Zhao (zhaoming02@hotmail.com)

Research

Keywords: Bone marrow mesenchymal stem cells, Erythropoietin, Acute kidney injury, SIRT1, Lung entrapment

Posted Date: June 2nd, 2020

DOI: https://doi.org/10.21203/rs.3.rs-17590/v2

Version of Record: A version of this preprint was published on November 16th, 2020. See the published version at https://doi.org/10.1186/s13578-020-00492-2.

Abstract

Background: Mesenchymal stem cells (MSCs) represent a promising treatment option for acute kidney injury (AKI). The main drawbacks of MSCs therapy, including the lack of specific homing after systemic infusion and early cell death in the inflammatory microenvironment, directly affect the therapeutic efficacy of MSCs. Erythropoietin (EPO)-preconditioning of MSCs promotes their therapeutic effect; however, the underlying mechanism remains unknown. In this study, we sought to investigate the efficacy and mechanism of EPO in bone marrow mesenchymal stem cells (BMSCs) for AKI treatment.

Results: We found that incubation of BMSCs with ischemia/reperfusion(I/R)-induced AKI kidney homogenate supernatant (KHS) caused apoptosis in BMSCs, which was decreased by EPO pretreatment, indicating that EPO protected the cells from apoptosis. Further, we showed that EPO up-regulated SIRT1 and Bcl-2 expression and down-regulated p53 expression. This effect was partially reversed by SIRT1 siRNA intervention. The anti-apoptotic effect of EPO in pretreated BMSCs may be mediated through the SIRT1 pathway. In a rat AKI model, 24 h after intravenous infusion, GFP-BMSCs were predominantly located in the lungs. However, EPO pretreatment reduced the lung entrapment of BMSCs and increased their distribution in the target organs. AKI rats infused with EPO-BMSCs had significantly lower levels of serum IL-1β and TNF-α, and a significantly higher level of IL-10 as compared to rats infused with untreated BMSCs. The administration of EPO-BMSCs after reperfusion reduced serum creatinine, blood urea nitrogen, and pathological scores in I/R-AKI rats more effectively than BMSCs treatment did.

Conclusions: Our data suggest that EPO pretreatment enhances the efficacy of BMSCs to improve the renal function and pathological presentation of I/R-AKI rats.

Background

Acute kidney injury (AKI) is one of the most clinically impactful diseases with high morbidity and mortality [1, 2]. Multiple injuries such as those resulting from sepsis, ischemia/reperfusion (I/R), and drug administration may induce AKI. I/R injury is a major cause of human AKI, which is associated with tubular necrosis, cast formation, tubular dilation, loss of brush border, and inflammation [3]. AKI remains a worldwide public health concern due to the increased risk of subsequent development of chronic kidney disease (CKD) [4]. The annual medical expenses associated with AKI treatment places a heavy burden on the public health care system, and yet AKI lacks an established treatment strategy. Therefore, there is an urgent need to find innovative and effective therapeutic strategies for treating AKI. The application of mesenchymal stem cells (MSCs) has been suggested as a promising treatment strategy for AKI [5, 6].

In recent years, MSCs have become an area of intense research in the field of stem cell therapy. MSCs are adherent, fibroblast-like cells derived from different tissues and organs, including bone marrow, umbilical cord blood, adipose tissue, and solid organs that have the potential for multidirectional differentiation and self-renewal. The tissue reparative/regenerative and immunoregulatory properties of MSCs render them as promising candidates for cell therapy and tissue regeneration. A large number of basic science

studies and clinical trials have demonstrated the safety, feasibility, and effectiveness of MSCs in the treatment of myocardial infarction, spinal cord injury, diabetes, and kidney disease [7-9]. MSCs exhibit renoprotective effects in both acute and chronic kidney injury. These effects seem to be associated with immunomodulation, anti-apoptotic effects, and reduction of disease-related inflammation [10, 11].

The main drawbacks of MSCs therapy are early pulmonary entrapment and the lack of specific homing to target tissues following systemic infusion [12, 13]. Even when the MSCs reach the target organ, many of the cells undergo apoptosis mainly due to the inhospitable local microenvironmental conditions, such as hypoxia, oxidative stress, and inflammation, which directly affect the therapeutic efficacy of MSCs [14, 15]. Application of pretreated MSCs is a novel strategy to enhance the capacity of MSCs to migrate and promote tissue repair in AKI [16, 17]. In our previous study, we demonstrated that pretreatment with 500 IU/ml erythropoietin (EPO) for 48 h prior to infusion markedly increased the homing and healing abilities of bone marrow-derived mesenchymal stem cells (BMSCs). These BMSCs significantly inhibited the apoptosis induced by cyclosporine A (CsA) toxicity in HK2 cells. Moreover, the single infusion treatment with EPO-BMSCs significantly improved the renal function in CsA-induced chronic toxic renal injury, and promoted the repair of renal fibrosis in rats [18].

EPO has been reported to stimulate the silent information regulator 1 (SIRT1) pathway, thereby promoting mitochondrial function and protecting white adipose tissue from oxidative stress [19]. EPO has also been demonstrated to inhibit doxorubicin (DOX)-induced cardiotoxicity by activating SIRT1 and enhancing mitochondrial function [20]. SIRT1 is a nicotinamide adenine dinucleotide (NAD+)-dependent protein deacetylase that plays an important role in maintaining the self-renewal and differentiation of MSCs, especially under stress conditions[21, 22]. SIRT1 also exhibits positive effects on senescence and apoptosis of MSCs [23, 24].

In this study, we sought to investigate the efficacy and mechanism of EPO pretreatment on BMSCs for the treatment of AKI. We demonstrate that EPO promotes the survival of transplanted BMSCs in an inflammatory microenvironment by stimulating the SIRT1-dependent pathway.

Results

Cell culture and characterization of BMSCs

BMSCs were transduced with a lentiviral vector expressing the green fluorescent protein (GFP) gene (GFP-BMSCs) and verified to retain stable GFP expression after proliferation. The passage 8 (P8) GFP-BMSCs were observed under a fluorescence microscope (Fig. 1A). Both untreated and EPO-treated GFP-BMSCs were capable of osteogenic and adipogenic differentiation when cultured in the appropriate inducing media. After three weeks of incubation, GFP-BMSCs and EPO-pretreated GFP-BMSCs differentiated into osteoblasts and adipocytes (Fig. 1B). Flow cytometric analysis confirmed that both groups of cells were CD45-negative but positive for the phenotypic markers CD90 and CD44 (Fig. 1C). Both groups of cells maintained their stem cell characteristics.

AKI-KHS-induced apoptosis in BMSCs

To study the anti-apoptotic effect of EPO on BMSCs, we pretreated BMSCs with EPO. BMSCs, EPO-BMSCs, EPO-BMSCs+SIRT1 siRNA, and EPO-BMSCs+Con siRNA were incubated with AKI-KHS (or N-KHS). After culture for 24 h, flow cytometric analysis was performed to assess apoptosis in each group (Fig. 2A). The apoptotic rates were significantly higher in the BMSCs+AKI-KHS and EPO-BMSCs+AKI-KHS groups when compared with that of the control group. AKI-KHS induced apoptosis in BMSCs, but EPO pretreatment protected the cells from this apoptotic effect. The anti-apoptotic effect of EPO was partially reversed by SIRT1 siRNA intervention. The apoptotic rate in the EPO-BMSCs+AKI-KHS group was significantly lower than that in the BMSCs+AKI-KHS group, whereas the rate in the EPO-BMSCs+AKI-KHS+SIRT1 siRNA group was significantly higher than that in the EPO-BMSCs+AKI-KHS group. (Fig. 2B).

Western blot analysis

Results of the flow cytometric analysis demonstrated that AKI-KHS treatment had an adverse effect on the survival of BMSCs, whereas EPO pretreatment improved BMSCs survival in the AKI microenvironment. To further investigate the anti-apoptotic mechanism of EPO, we analyzed the expression of the anti-apoptotic factor, Bcl-2, the pro-apoptotic factor, p53, and SIRT1. All cytokines were examined using western blot analysis (Fig. 3A). The expression of SIRT1 and Bcl-2 in the EPO-BMSCs+AKI-KHS group was significantly increased compared with that in the BMSCs+AKI-KHS group ($p < 0.05$), and the expression of p53 was significantly higher in the BMSCs+AKI-KHS group than in the EPO-BMSCs+AKI-KHS group ($p < 0.05$) . The effect of EPO on the expression of SIRT1, Bcl-2, and p53 was partially reversed by SIRT1 siRNA intervention (Fig. 3B-D).

Treatment of AKI in rats

Blood biochemical indicators

To compare the effects of BMSCs and EPO-BMSCs on AKI rats, we measured the levels of blood urea nitrogen (BUN) and serum creatinine (SCr) on day 1 and 5 after treatment, and found that they were significantly increased. Treatment of AKI rats with EPO, BMSCs, and EPO-BMSCs showed varying therapeutic effects. All three treatments reduced the level of BUN and SCr on day 1 and 5 after treatment compared with that in the control group treated with the vehicle. However, only BMSCs and EPO-BMSCs treatment showed a significant effect ($p < 0.05$). Rats in the EPO-BMSCs group had significantly lower BUN and SCr levels than those in the BMSCs group ($p < 0.05$, Fig. 3A and B).

Detection of cytokines

Twenty-four hours after the treatment of AKI rats with vehicle, EPO, BMSCs, and EPO-BMSCs, the serum levels of the pro-inflammatory cytokines, IL-1β and TNF-α and the anti-inflammatory cytokine IL-10 were determined using enzyme-linked immunosorbent assay (ELISA). There was a significant increase in the level of IL-1β, TNF-α, and IL-10 one day after the induction of AKI. The serum levels of the cytokines in the EPO group did not significantly differ from those in the model group. Infusion of BMSCs significantly

reduced the serum levels of IL-1β (Fig. 3C) and TNF-α (Fig. 3D), whereas the level of IL-10 was increased(Fig. 3E). Furthermore, AKI rats that underwent EPO-BMSCs infusion had significantly lower serum IL-1β and TNF-α levels and a significantly higher IL-10 serum level than those in AKI rats that received BMSCs infusion (Fig. 3C-E).

GFP fluorescence in frozen sections

Our data showed that 24 h after intravenous infusion, a majority of the GFP-BMSCs were trapped in the lungs, with minimal fluorescence detected in the spleen, liver, and kidneys. In the GFP-EPO-BMSCs group, the fluorescence intensity was significantly lower in the lungs but higher in other organs, especially the kidneys, compared with the corresponding fluorescence intensities in the GFP-BMSCs group. GFP-BMSCs and GFP-EPO-BMSCs were predominantly detected in the lungs, but EPO preconditioning reduced the lung entrapment of BMSCs and increased their distribution in the target organs (Fig. 4).

Histological analysis

Hematoxylin and eosin (HE) staining of kidney sections revealed tubular necrosis, cast formation, tubular dilation, and loss of brush border in the AKI model group (Fig. 5A). These pathological injuries were assessed using the pathological scores obtained after treatment with EPO, BMSCs, and EPO-BMSCs on day 1 and 5. The pathological scores in the BMSCs and EPO-BMSCs treatment groups were significantly lower than those in the model group one and five days after treatment ($p < 0.05$). Both BMSCs and EPO-BMSCs infusion reduced tubular injury; however, EPO-BMSCs administration improved tubular injury significantly more on day 5 as compared to infusion with BMSCs (Fig. 5B).

Discussion

In the present study, we reveal novel insights regarding the efficacy and mechanism of EPO-BMSCs in I/R-AKI. Our findings showed that I/R-AKI microenvironment caused apoptosis in BMSCs, but EPO pretreatment protected the cells from this apoptotic effect. We found that EPO up-regulated SIRT1 and Bcl-2 expression and down-regulated p53 expression in the AKI model. The anti-apoptotic effect of EPO may be mediated through the SIRT1 pathway. EPO pretreatment reduced pulmonary entrapment of BMSCs and increased the number of cells reaching the target organs. Furthermore, EPO pretreatment reduced the expression of disease-related inflammatory cytokines. AKI rats that underwent EPO-BMSCs infusion had significantly lower serum IL-1β and TNF-α levels, and a significantly higher IL-10 level than those in rats treated with BMSCs. Our data suggest that EPO pretreatment enhances the efficacy of BMSCs to improve renal function and pathological presentation of I/R-AKI rats.

The protective effect of MSCs in acute and chronic renal injury may be through a paracrine/autocrine mechanism, which is related to immune regulation, anti-apoptosis, and reduction of disease-related inflammation. Several studies have shown that the survival and retention of MSCs in target organs or tissues is closely related to the therapeutic effect mediated by MSCs. The main drawbacks of MSCs therapy are the early pulmonary entrapment and the lack of specific homing after systemic infusion.

Most of the MSCs undergo cell death after transplantation, mainly due to an adverse microenvironment, directly affecting the therapeutic efficacy of MSCs [14, 15].

Increasing the dose of MSCs infused represents a viable option to achieve better therapeutic effects; however, this is accompanied by some side effects, such as microvascular embolization and the potential risk of long-term tumor growth. Therefore, current studies on MSCs-related therapies have focused on lower infusion doses to achieve the greatest therapeutic effect possible. Cell-free treatments, including microvesicles, exosomes, specific cytokines, miRNA, and the pretreatment of MSCs, represent viable alternatives to address the issue of long-term negative effects [25-27]. Pretreating MSCs is a novel strategy to enhance the capacity of MSCs to migrate and promote tissue repair in injured kidneys [28]. Pretreatment, before infusion, with cytokines such as transforming growth factor β1 (TGF-β1), interleukin-17A (IL-17A), and melatonin can increase the number of MSCs homing to the injured kidney, promote the recovery of renal function, and ameliorate renal impairments [3, 17, 29]. Similar results were obtained upon pretreating MSCs with EPO.

EPO is a glycoprotein hormone that promotes the proliferation and differentiation of bone marrow hematopoietic stem cells and the hematopoietic function of bone marrow through EPO receptor (EpoR) signaling. BMSCs and bone marrow HSCs are homologous and express EpoR. However, many other cell types, including neurons, endothelial cells, cardiomyocytes, and renal tubular cells also express the EpoR and respond to EPO treatment [30]. Studies have shown that EPO is suitable for the treatment of a variety of diseases, including cerebral ischemia, myocardial infarction, chronic congestive heart failure, and renal injury [20, 31]. Moreover, some studies suggest that overexpression of EPO in MSCs by gene-transfection could further enhance the therapy effect of MSCs[32, 33]. Compared with other pretreatments or strategies that improve the therapeutic effect of MSCs, the *in vitro* pretreatment with EPO has significant advantages in terms of clinical feasibility. First, EPO is a commonly used therapeutic drug with few side effects and is widely used in the clinical treatment of anemia, especially in patients with CKD. Second, it exhibits anti-oxidative and anti-inflammatory effects.

Our data showed that 24 h following intravenous infusion, GFP-BMSCs were predominantly located in the lungs. EPO preconditioning reduced the entrapment of BMSCs in the lungs and increased the distribution of GFP-BMSCs in the target organs. In our previous study, we showed that the pretreatment of BMSCs with an optimal concentration of EPO for an appropriate time induced a marked change in the proliferation rate and cytoskeletal rearrangement of BMSCs. After incubation with EPO, most of the cells exhibited parallelly-oriented filaments organized along the cell axis. We observed that C-X-C chemokine receptor type 4 (CXCR4), a pivotal mediator of migration and engraftment in MSCs, was up-regulated following EPO treatment, enhancing the migration ability of BMSCs [18].

Homing of MSCs to injured tissues is very critical in cell therapy. Various methods to apply MSCs exist, such as peripheral intravenous infusion, arterial infusion to the target organ, and local injection. Local injection increases the risk of bleeding and tissue injury, while direct arterial administration can result in occlusion and embolization of the target organs. Therefore, MSCs are mostly administered through a

standard intravenous route. Pulmonary entrapment is a major problem after intravenous infusion of MSCs. Harting et al. demonstrated that less than 4% of the infused cells were likely to traverse the pulmonary microvasculature and reach the arterial circulation, a phenomenon termed "pulmonary first-pass effect", which limits the efficacy of this therapeutic approach [34]. Some studies show that small microspheres (4–5 μm) could pass through the pulmonary system, whereas the majority of the large microspheres (20-μm) and MSCs (15–19 μm) are trapped within the lungs. Lung entrapment may be due to the small capillary size, large capillary network of the lungs, and strong adhesion properties of MSCs [35-37]. A variety of molecules may be involved in lung entrapment of systemically infused cells, and the composition of cell surface molecules, such as α4, α5, and α6 integrins, may affect the migratory behavior of the therapeutic cells [13, 37]. We found that after intravenous infusion, most of the stem cells were trapped within the lungs, but EPO pretreatment reduced pulmonary entrapment and increased the number of cells reaching the target organ.

We also found that EPO up-regulated SIRT1 and Bcl-2 expression and down-regulated p53 expression. SIRT1 is an NAD^+-dependent deacetylase belonging to class Ⅲ histone deacetylases and is known as the longevity protein in mammals. SIRT1 regulates a variety of cellular signaling pathways by modifying the acetylation status of target proteins including p53, members of the forkhead family of transcription factors (FOXO), and nuclear factor NF-κB. Following activation, SIRT1 participates in a plethora of cellular processes such as cell senescence, apoptosis, DNA damage repair, cell cycle, oxidative stress response, energy metabolism regulation, tumor generation, and other physiological and pathological processes [38-40]. Tumor suppressor protein, p53, plays a vital role in apoptotic signaling pathways, including membrane and mitochondrial apoptotic pathways, and affects the transcription and expression of many apoptosis-related cytokines in the nucleus [41]. SIRT1 reduces the transcriptional activity of p53 and inhibits p53-dependent cell apoptosis, caused by DNA damage [42]. In tumor studies, SIRT1 inhibited apoptosis in tumor cells by regulating p53 and Bcl-2 [43]. EPO has been demonstrated to impede DOX-induced cardiotoxicity by activating SIRT1, leading to enhancement of mitochondrial function [20]. Hong et al. revealed that EPO alleviates hepatic steatosis by activating autophagy through SIRT1-dependent de-acetylation of LC3 [38]. In our study, most of the BMSCs undergo cell death after transplantation, mainly due to the adverse local microenvironment. Therefore, improving cell survival and retention of BMSCs is pertinent to promote their therapeutic efficacy in AKI therapy. The observed beneficial effect of EPO pretreatment was associated with SIRT1 signaling activation, leading to the de-acetylation and subsequent inactivation of p53 and up-regulation of Bcl-2 expression, which in turn reduces apoptosis in BMSCs. These findings, therefore, demonstrate that the anti-apoptotic effect following EPO pretreatment of BMSCs may be mediated though the SIRT1 pathway.

The mechanism by which EPO-pretreated BMSCs accelerate the repair of AKI includes three facets. First, after incubation with EPO, most of the BMSCs exhibited parallelly oriented filaments organized along the cell axis and showed increased CXCR4 expression. These changes reduced the lung entrapment of BMSCs and increased their homing to target organs. Second, EPO up-regulated SIRT1 and Bcl-2 expression, and down-regulated p53 expression in BMSCs. SIRT1 inhibited apoptosis in BMSCs by

regulating p53 and Bcl-2 expression. Third, the direct anti-inflammatory effect of EPO-BMSCs is also likely to be involved in the process. However, the present study has some limitations and did not elucidate the mechanism underlying EPO-mediated activation of SIRT1 signaling in BMSCs, which requires future investigations.

Conclusion

In conclusion, EPO-BMSCs were more effective in reducing the levels of SCr and BUN, and the pathological scores in I/R-AKI rats after reperfusion when compared to untreated BMSCs. These results suggest that EPO pretreatment may potentially be a novel alternative to untreated BMSCs for the management of AKI.

Materials And Methods

Cell culture

Sprague–Dawley (SD)-derived BMSCs (P5) (Cyagen Biosciences Inc., Guangzhou, China) that stably express GFP were cultured in Dulbecco's Modified Eagle Medium (DMEM, Gibco, Carlsbad, CA, USA) containing 10% fetal bovine serum (FBS, Gibco) and 1% antibiotics (50 U/ml penicillin and 50 μg/ml streptomycin, Gibco) at 37 °C and 5% CO_2. The P8-GFP-BMSCs were used for *in vivo* and *in vitro* experiments.

Characterization of BMSCs incubated with EPO

GFP-BMSCs were trypsinized after incubation with or without EPO (500 IU/ml) for 48 h and washed three times with phosphate-buffered saline (PBS). Cell surface markers were examined by immunostaining with the following antibodies: phycoerythrin (PE)-conjugated anti-CD45 (BD Biosciences, San Jose, CA), fluorescein isothiocyanate (FITC)-conjugated anti-CD44 (BD Biosciences), and FITC-conjugated anti-CD90 (BD Biosciences) antibody. The labeled cells were analyzed using a flow cytometer (BD LSRFortessa™, Piscataway, NJ). Osteogenic and adipogenic differentiation potential of the cells in the two groups was examined according to the manufacturer's protocol (Cyagen, China).

I/R-AKI kidney homogenate supernatant (KHS) preparation

An AKI model was established using SD rats by clamping both renal pedicles for 45 min, followed by clamp-release to allow reperfusion. Both kidneys were harvested 60 min after reperfusion, cut into small pieces, and homogenized in PBS using a glass homogenizer to obtain a 20 g/l homogenate. The homogenate was then centrifuged at 20,000 rpm for 15 min at 4 ℃. The supernatant was filtered through a 30-μm mesh-sized disposable sterile filter to obtain AKI-KHS, which was stored at -80 ℃ until further use. Normal KHS (N-KHS) obtained from healthy SD rats was used as a control.

SiRNA transfection

Cells were transiently transfected with SIRT1 siRNA or control siRNA using Lipofectamine RNAiMAX reagent (Life Technologies, Carlsbad, CA) according to the manufacturer's protocol. Cells were analyzed 36 h after siRNA transfection. The SIRT1 siRNA and control siRNA were synthesized by RiboBio technologies (RiboBio, Guangzhou, China). The sequence of SIRT1 siRNA was as follows: 5¢-CACCUGAGUUGGAUGAUAUTT-3¢ (sense) and 5¢-AUAUCAUCCAACUAGGUGTT-3¢ (antisense).

Anti-apoptotic effect of BMSCs pretreated with EPO

To study the anti-apoptotic effect of BMSCs pretreated with EPO, we incubated BMSCs and EPO-BMSCs with AKI-KHS (or N-KHS). Cells were seeded at 4 x 10^5 cells/well in 6-well plates containing DMEM/F12 with 2% FBS. Transwell chambers with 0.4 μm pore size polycarbonate filters (Corning Incorporated, NY, USA) were inserted into the wells for intervention. Five groups were set up: the control BMSCs+N-KHS group, (BMSCs were plated in 6-well plates and 1.5 ml N-KHS was added to the upper chamber); the BMSCs+AKI-KHS group (BMSCs were plated in 6-well plates and 1.5 ml AKI-KHS was added to the upper chamber); the EPO-BMSCs+AKI-KHS group (EPO-BMSCs were plated in 6-well plates and 1.5 ml AKI-KHS was added to the upper chamber); the EPO-BMSCs+AKI-KHS+SIRT1 siRNA group (EPO-BMSCs transfected with SIRT1 siRNA were plated in 6-well plates and 1.5 ml AKI-KHS was added to the upper chamber); and the EPO-BMSCs+AKI-KHS+Con siRNA group (EPO-BMSCs transfected with control siRNA were plated in 6-well plates and 1.5 ml AKI-KHS was added to the upper chamber). All groups were incubated at 37 ℃ for 24 h in a humidified atmosphere of 5% CO2. The Annexin V-FITC apoptosis detection kit (Invitrogen, Frederick, MD, USA) was used to detect apoptotic cells according to the manufacturer's protocol. Apoptosis in BMSCs and EPO-BMSCs was then analyzed by flow cytometry; cells were subsequently harvested for western blot analysis.

Western blotting

After each treatment, the cells were washed twice with PBS, harvested, and the proteins were extracted. The following antibodies were used to analyze protein expression: anti-BCL-2 (1:1000, Santa Cruz, CA), p53 (1:1000, Santa Cruz), SIRT1 (1:1000, Santa Cruz), and anti-β-actin (1:2000, Bioworld, Shanghai, China). Protein bands were quantified by densitometry using an Alpha Innotech imaging system. Protein levels were normalized to β-actin expression using Image J analysis software.

Animals

Adult female SD rats (200–250 g), purchased from the animal house of the Faculty of Medicine at Southern Medical University (Guangzhou, China), were used for the study. Animals were housed under specific pathogen-free conditions with a 12 h dark-light cycle and supplied with pelleted food and tap water ad libitum. Animals were allowed to acclimatize to the housing conditions for one week. All procedures were performed in strict accordance with the Guidelines for Animal Experimentation of Southern Medical University (Guangzhou, China).

Animal grouping and treatment

AKI models were established using SD rats. The animals were anesthetized by intraperitoneal injection of 2% sodium pentobarbital (50 mg/kg). Abdominal incisions were made, and the two renal pedicles were bluntly separated. A microvascular clamp was used to clamp both renal pedicles for 45 min, followed by clamp-release to allow reperfusion. Then, the abdominal incision was closed. Intervention treatments were administered to rats through tail vein injection after reperfusion.

To determine the effects of BMSCs and EPO-BMSCs treatment, we randomly divided the rats (n = 50) into the following five groups (10 rats per group): sham group (kidneys of the SD rats were exposed for 45 min and 1 ml low-glucose DMEM was injected), model group (both renal pedicles were clamped for 45 min and 1 ml low-glucose DMEM was injected), EPO group (both renal pedicles were clamped for 45 min and 1 ml EPO (500 IU/ml) was injected), BMSCs group (both renal pedicles were clamped for 45 min and 1 x 10^6 BMSCs were injected), and EPO-BMSCs group (both renal pedicles were clamped for 45 min and 1 x 10^6 EPO-BMSCs were injected). All rats were housed at a favorable temperature and humidity (a temperature of 21 °C ±2°C, and a humidity of 55 % ±5 %) with an unlimited supply of water and food post-surgery. Rats were sacrificed one and five days after treatment (five rats at each time point). Blood samples and tissues from the kidneys, lung, spleen, and liver were collected for subsequent experiments. Blood samples were collected through the inferior vena cava, and serum was separated and stored at -80 °C until use. Both kidneys of each rat were immediately excised and cut into two coronal sections. The sections were fixed in 4% paraformaldehyde at room temperature. In the BMSCs and EPO-BMSCs group, the lung, spleen, liver, and the remaining part of the kidney were immediately analyzed.

Renal functional analysis

Renal function was estimated using diagnostic kits. SCr was measured using a colorimetric microplate assay based on the Jaffe reaction (Quantichrom Creatinine Assay; BioAssay Systems). BUN was measured using a colorimetric assay kit according to the manufacturer's instructions (Quantichrom Urea Assay; BioAssay Systems).

ELISA

Serum concentrations of the inflammatory factors IL-1β and TNF-α and the anti-inflammatory cytokine IL-10 were measured by ELISA (R&D Systems, Minneapolis, MN, USA). The assay was performed according to the manufacturer's instructions.

GFP fluorescence in frozen tissue sections

To verify the *in vivo* distribution of BMSCs after intravenous infusion, we prepared fast-frozen sections from the kidney, lung, spleen, and liver 24 h after GFP-BMSCs and GFP-EPO-BMSCs infusion. We immediately observed the sections under a fluorescence microscope.

Renal histological analysis

To detect kidney injuries, we fixed the samples in 4% neutral-buffered paraformaldehyde for histological assessment, embedded them in paraffin, and cut them in 3-μm-thick slices. The sections were then stained with HE (Servicebio, China). Histological examinations were performed in a blinded manner for acute tubular necrosis (ATN) scores regarding the grading of tubular necrosis, cast formation, tubular dilation, and loss of brush border. Ten non-overlapping fields (×200) were randomly selected and scored as follows: 0, no damage; 1, patchy isolated necrosis ≤ 10%; 2, tubular necrosis between 10% and 25%; 3, tubular necrosis between 25% and 50%; 4, tubular necrosis > 50% [3].

Statistical analysis

Results are expressed as mean ± standard deviation. Student's *t* test was performed to analyze the differences between two groups. Multiple-group comparison was performed using one-way analysis of variance (ANOVA) test. SPSS 19.0 statistical software was used for statistical analysis. $P < 0.05$ was considered statistically significant.

Declarations

Authors contributions

SZ designed the overall study, executed the experiments, analyzed data, and wrote the manuscript; YMQ executed the experiments, prepared the manuscript; YGL designed the overall study, supervised the project and edited the manuscript; DL,JMH,JL,ML,YG,LPF,LYL provided suggestions for the project and edited the manuscript. MZ: designed the overall study, analyzed data and final approval of manuscript. All authors read and approved the final manuscript.

Ethics approval and consent to participate

Not applicable.

Availability of data and material

Not applicable.

Competing Interests

The authors declare that they have no conflicts of interests.

Consent for publication

Not applicable.

Funding

This work was supported by the Initiative Research Projects of Southern Medical University in 2018(No. PY2018N049).

Acknowledgments

Not applicable.

Author details

[1]Department of Organ Transplantation, Zhujiang Hospital, Southern Medical University, No.253, Industrial Avenue, Haizhu District, Guangzhou 510280, Guangdong Province, China;

References

1. Chawla LS, Bellomo R, Bihorac A, Goldstein SL, Siew ED, Bagshaw SM, Bittleman D*, et al*. Acute kidney disease and renal recovery: consensus report of the Acute Disease Quality Initiative (ADQI) 16 Workgroup. *Nature reviews Nephrology.* 2017;13:241-57.
2. Xu X, Nie S, Liu Z, Chen C, Xu G, Zha Y, Qian J*, et al*. Epidemiology and Clinical Correlates of AKI in Chinese Hospitalized Adults. *Clinical journal of the American Society of Nephrology : CJASN.* 2015;10:1510-8.
3. Bai M, Zhang L, Fu B, Bai J, Zhang Y, Cai G, Bai X*, et al*. IL-17A improves the efficacy of mesenchymal stem cells in ischemic-reperfusion renal injury by increasing Treg percentages by the COX-2/PGE2 pathway. *Kidney Int.* 2018;93:814-25.
4. Liu J, Kumar S, Dolzhenko E, Alvarado GF, Guo J, Lu C, Chen Y*, et al*. Molecular characterization of the transition from acute to chronic kidney injury following ischemia/reperfusion. *JCI insight.* 2017;2:
5. Xiang J, Jiang T, Zhang W, Xie W, Tang X, Zhang J. Human umbilical cord-derived mesenchymal stem cells enhanced HK-2 cell autophagy through MicroRNA-145 by inhibiting the PI3K/AKT/mTOR signaling pathway. *Exp Cell Res.* 2019;378:198-205.
6. Rota C, Morigi M, Imberti B. Stem Cell Therapies in Kidney Diseases: Progress and Challenges. *Int J Mol Sci.* 2019;20:
7. Quijada P, Salunga HT, Hariharan N, Cubillo JD, El-Sayed FG, Moshref M, Bala KM*, et al*. Cardiac Stem Cell Hybrids Enhance Myocardial Repair. *Circ Res.* 2015;117:695-706.
8. Sun Q, Huang Z, Han F, Zhao M, Cao R, Zhao D, Hong L*, et al*. Allogeneic mesenchymal stem cells as induction therapy are safe and feasible in renal allografts: pilot results of a multicenter randomized controlled trial. *J Transl Med.* 2018;16:52.
9. Savukinas UB, Enes SR, Sjöland AA, Westergren-Thorsson G. Concise Review: The Bystander Effect: Mesenchymal Stem Cell-Mediated Lung Repair. *Stem cells (Dayton, Ohio).* 2016;34:1437-44.
10. Aghajani Nargesi A, Lerman LO, Eirin A. Mesenchymal stem cell-derived extracellular vesicles for kidney repair: current status and looming challenges. *Stem Cell Res Ther.* 2017;8:273.
11. Roushandeh AM, Bahadori M, Roudkenar MH. Mesenchymal Stem Cell-based Therapy as a New Horizon for Kidney Injuries. *Arch Med Res.* 2017;48:133-46.

12. Mäkelä T, Takalo R, Arvola O, Haapanen H, Yannopoulos F, Blanco R, Ahvenjärvi L*, et al*. Safety and biodistribution study of bone marrow-derived mesenchymal stromal cells and mononuclear cells and the impact of the administration route in an intact porcine model. *Cytotherapy.* 2015;17:392-402.
13. Wang S, Guo L, Ge J, Yu L, Cai T, Tian R, Jiang Y*, et al*. Excess Integrins Cause Lung Entrapment of Mesenchymal Stem Cells. *Stem cells (Dayton, Ohio).* 2015;33:3315-26.
14. El-Magd MA, Mohamed Y, El-Shetry ES, Elsayed SA, Abo Gazia M, Abdel-Aleem GA, Shafik NM*, et al*. Melatonin maximizes the therapeutic potential of non-preconditioned MSCs in a DEN-induced rat model of HCC. *Biomedicine & pharmacotherapy = Biomedecine & pharmacotherapie.* 2019;114:108732.
15. Li X, Shang B, Li YN, Shi Y, Shao C. IFNγ and TNFα synergistically induce apoptosis of mesenchymal stem/stromal cells via the induction of nitric oxide. *Stem Cell Res Ther.* 2019;10:18.
16. Zhao L, Hu C, Zhang P, Jiang H, Chen J. Novel preconditioning strategies for enhancing the migratory ability of mesenchymal stem cells in acute kidney injury. *Stem Cell Res Ther.* 2018;9:225.
17. Zhao L, Hu C, Zhang P, Jiang H, Chen J. Melatonin preconditioning is an effective strategy for mesenchymal stem cell-based therapy for kidney disease. *J Cell Mol Med.* 2020;24:25-33.
18. Zhou S, Liu YG, Zhang Y, Hu JM, Liu D, Chen H, Li M*, et al*. Bone mesenchymal stem cells pretreated with erythropoietin enhance the effect to ameliorate cyclosporine A-induced nephrotoxicity in rats. *J Cell Biochem.* 2018;119:8220-32.
19. Wang L, Teng R, Di L, Rogers H, Wu H, Kopp JB, Noguchi CT. PPARα and Sirt1 mediate erythropoietin action in increasing metabolic activity and browning of white adipocytes to protect against obesity and metabolic disorders. *Diabetes.* 2013;62:4122-31.
20. Cui L, Guo J, Zhang Q, Yin J, Li J, Zhou W, Zhang T*, et al*. Erythropoietin activates SIRT1 to protect human cardiomyocytes against doxorubicin-induced mitochondrial dysfunction and toxicity. *Toxicol Lett.* 2017;275:28-38.
21. Wang H, Lv C, Gu Y, Li Q, Xie L, Zhang H, Miao D*, et al*. Overexpressed Sirt1 in MSCs Promotes Dentin Formation in Bmi1-Deficient Mice. *J Dent Res.* 2018;97:1365-73.
22. Wang Y, Chen G, Yan J, Chen X, He F, Zhu C, Zhang J*, et al*. Upregulation of SIRT1 by Kartogenin Enhances Antioxidant Functions and Promotes Osteogenesis in Human Mesenchymal Stem Cells. *Oxid Med Cell Longev.* 2018;2018:1368142.
23. Liu X, Chen H, Zhu W, Chen H, Hu X, Jiang Z, Xu Y*, et al*. Transplantation of SIRT1-engineered aged mesenchymal stem cells improves cardiac function in a rat myocardial infarction model. *The Journal of heart and lung transplantation : the official publication of the International Society for Heart Transplantation.* 2014;33:1083-92.
24. Zhou L, Chen X, Liu T, Gong Y, Chen S, Pan G, Cui W*, et al*. Melatonin reverses H2 O2 -induced premature senescence in mesenchymal stem cells via the SIRT1-dependent pathway. *J Pineal Res.* 2015;59:190-205.
25. Sui BD, Hu CH, Liu AQ, Zheng CX, Xuan K, Jin Y. Stem cell-based bone regeneration in diseased microenvironments: Challenges and solutions. *Biomaterials.* 2019;196:18-30.

26. Grange C, Skovronova R, Marabese F, Bussolati B. Stem Cell-Derived Extracellular Vesicles and Kidney Regeneration. *Cells.* 2019;8:
27. Witwer KW, Van Balkom BWM, Bruno S, Choo A, Dominici M, Gimona M, Hill AF*, et al*. Defining mesenchymal stromal cell (MSC)-derived small extracellular vesicles for therapeutic applications. *Journal of extracellular vesicles.* 2019;8:1609206.
28. Zhao L, Hu C, Zhang P, Jiang H, Chen J. Preconditioning strategies for improving the survival rate and paracrine ability of mesenchymal stem cells in acute kidney injury. *J Cell Mol Med.* 2019;23:720-30.
29. Cai J, Jiao X, Zhao S, Liang Y, Ning Y, Shi Y, Fang Y*, et al*. Transforming growth factor-β1-overexpressing mesenchymal stromal cells induced local tolerance in rat renal ischemia/reperfusion injury. *Cytotherapy.* 2019;21:535-45.
30. Bi B, Guo J, Marlier A, Lin SR, Cantley LG. Erythropoietin expands a stromal cell population that can mediate renoprotection. *American journal of physiology Renal physiology.* 2008;295:F1017-22.
31. Jun JH, Jun NH, Shim JK, Shin EJ, Kwak YL. Erythropoietin protects myocardium against ischemia-reperfusion injury under moderate hyperglycemia. *Eur J Pharmacol.* 2014;745:1-9.
32. Feng J, Wang W. Hypoxia pretreatment and EPO-modification enhance the protective effects of MSC on neuron-like PC12 cells in a similar way. *Biochem Biophys Res Commun.* 2017;482:232-8.
33. Lin H, Luo X, Jin B, Shi H, Gong H. The Effect of EPO Gene Overexpression on Proliferation and Migration of Mouse Bone Marrow-Derived Mesenchymal Stem Cells. *Cell Biochem Biophys.* 2015;71:1365-72.
34. Harting MT, Jimenez F, Xue H, Fischer UM, Baumgartner J, Dash PK, Cox CS. Intravenous mesenchymal stem cell therapy for traumatic brain injury. *J Neurosurg.* 2009;110:1189-97.
35. Fischer UM, Harting MT, Jimenez F, Monzon-Posadas WO, Xue H, Savitz SI, Laine GA*, et al*. Pulmonary passage is a major obstacle for intravenous stem cell delivery: the pulmonary first-pass effect. *Stem cells and development.* 2009;18:683-92.
36. Lipowsky HH, Bowers DT, Banik BL, Brown JL. Mesenchymal Stem Cell Deformability and Implications for Microvascular Sequestration. *Ann Biomed Eng.* 2018;46:640-54.
37. Nystedt J, Anderson H, Tikkanen J, Pietilä M, Hirvonen T, Takalo R, Heiskanen A*, et al*. Cell surface structures influence lung clearance rate of systemically infused mesenchymal stromal cells. *Stem cells (Dayton, Ohio).* 2013;31:317-26.
38. Hong T, Ge Z, Meng R, Wang H, Zhang P, Tang S, Lu J*, et al*. Erythropoietin alleviates hepatic steatosis by activating SIRT1-mediated autophagy. *Biochimica et biophysica acta Molecular and cell biology of lipids.* 2018;1863:595-603.
39. Sun W, Qiao W, Zhou B, Hu Z, Yan Q, Wu J, Wang R*, et al*. Overexpression of Sirt1 in mesenchymal stem cells protects against bone loss in mice by FOXO3a deacetylation and oxidative stress inhibition. *Metabolism.* 2018;88:61-71.
40. Yoon DS, Choi Y, Lee JW. Cellular localization of NRF2 determines the self-renewal and osteogenic differentiation potential of human MSCs via the P53-SIRT1 axis. *Cell Death Dis.* 2016;7:e2093.

41. Mai WX, Gosa L, Daniels VW, Ta L, Tsang JE, Higgins B, Gilmore WB, *et al*. Cytoplasmic p53 couples oncogene-driven glucose metabolism to apoptosis and is a therapeutic target in glioblastoma. *Nat Med.* 2017;23:1342-51.
42. Conrad E, Polonio-Vallon T, Meister M, Matt S, Bitomsky N, Herbel C, Liebl M, *et al*. HIPK2 restricts SIRT1 activity upon severe DNA damage by a phosphorylation-controlled mechanism. *Cell Death Differ.* 2016;23:110-22.
43. Lin XL, Li K, Yang Z, Chen B, Zhang T. Dulcitol suppresses proliferation and migration of hepatocellular carcinoma via regulating SIRT1/p53 pathway. *Phytomedicine : international journal of phytotherapy and phytopharmacology.* 2020;66:153112.

Figures

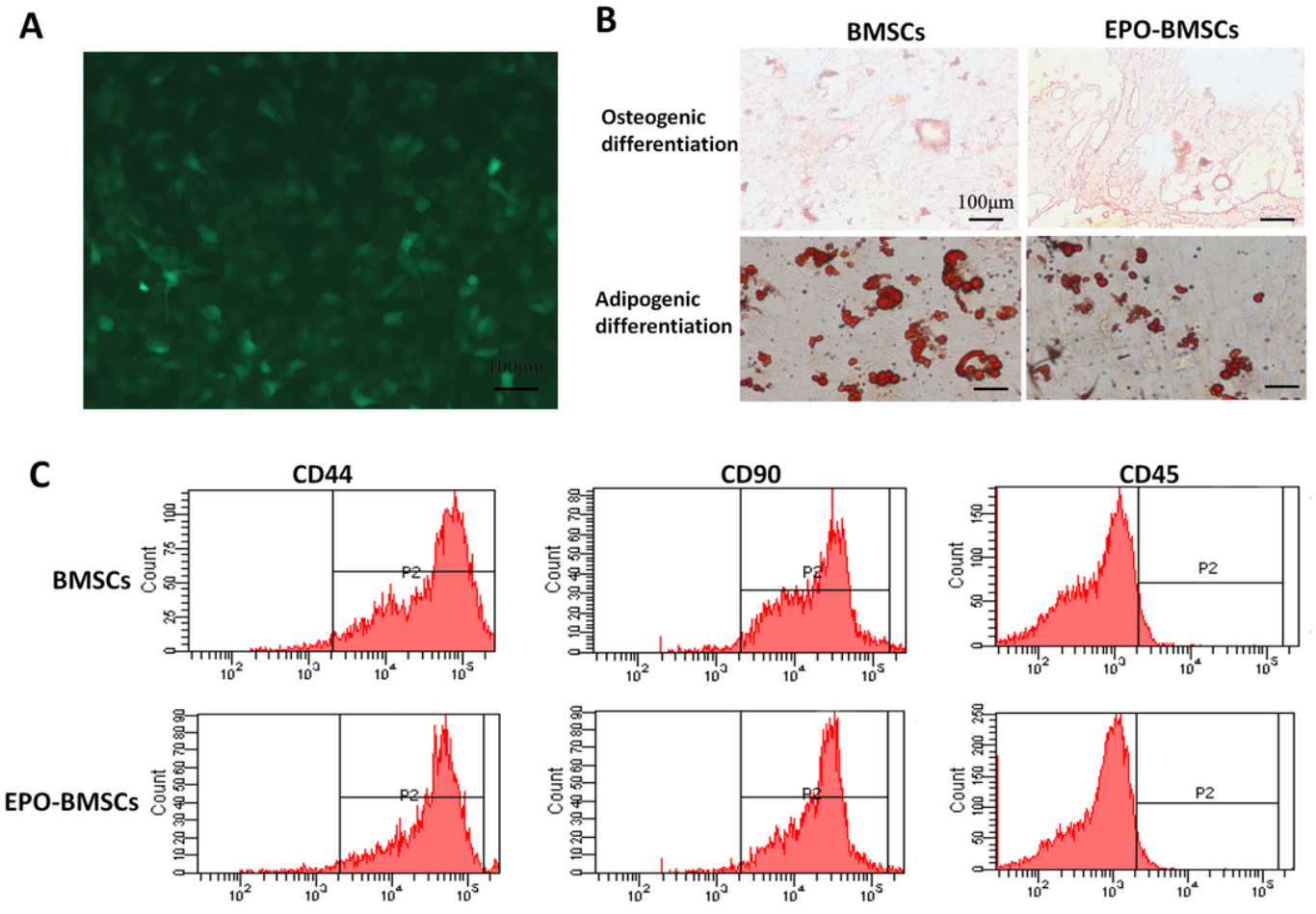

Figure 1

Cell culture and characterization of BMSCs. (A) Image of P8 GFP-BMSCs as observed under fluorescent microscope. (B) GFP-BMSCs and EPO-pretreated GFP-BMSCs differentiated into osteoblasts and adipocytes. (C) Flow cytometric analysis confirmed that untreated and EPO-treated cells were CD45-negative and positive for the phenotypic markers CD90 and CD44.

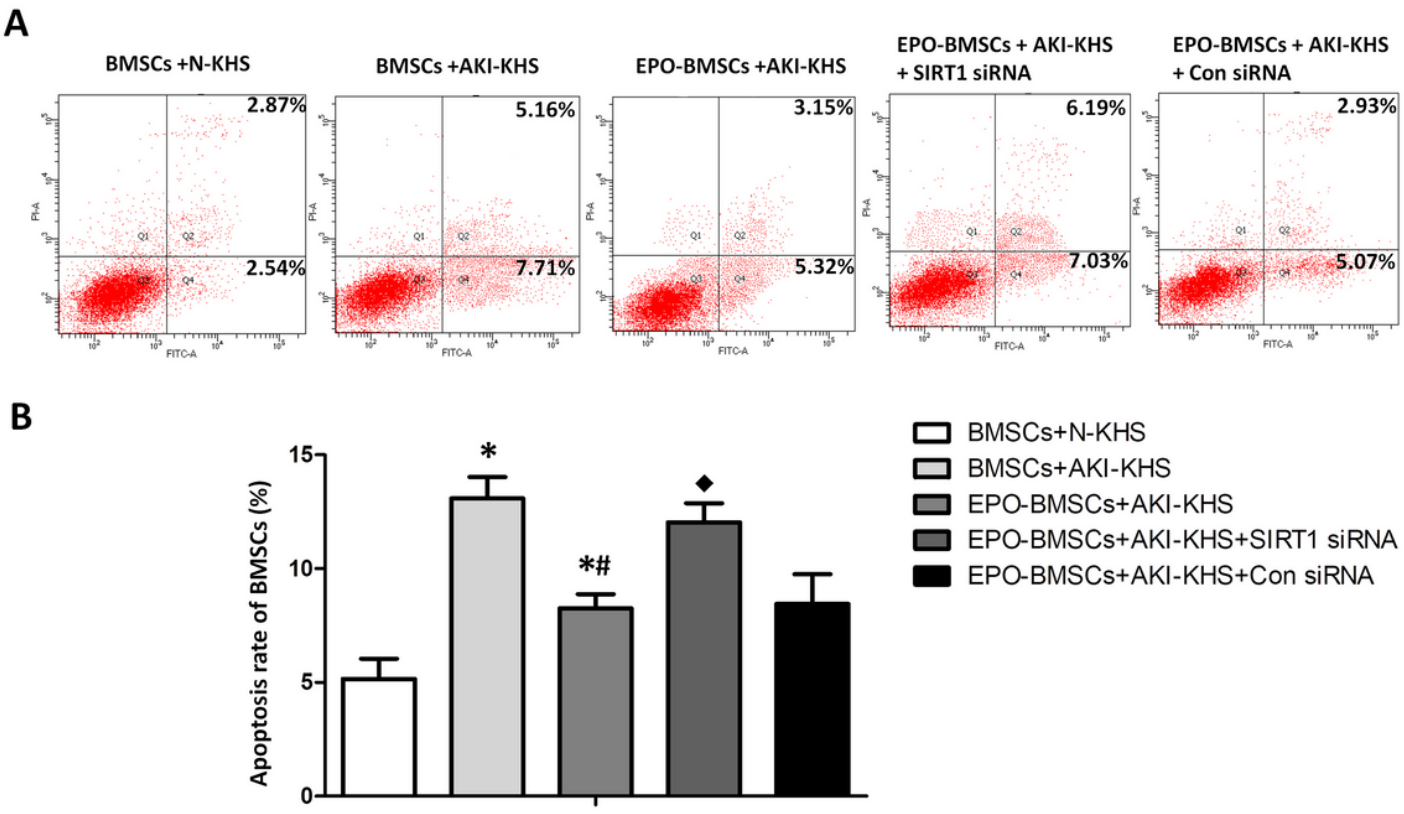

Figure 2

AKI-KHS induced apoptosis in BMSCs. (A) Flow cytometric analysis was performed 24 h after culturing to assess apoptosis in each group. (B) Apoptotic rates in each group. *p < 0.05 versus BMSCs+N-KHS, #p < 0.05 versus BMSCs+AKI-KHS, ◆p< 0.05 versus EPO-BMSCs+AKI-KHS.

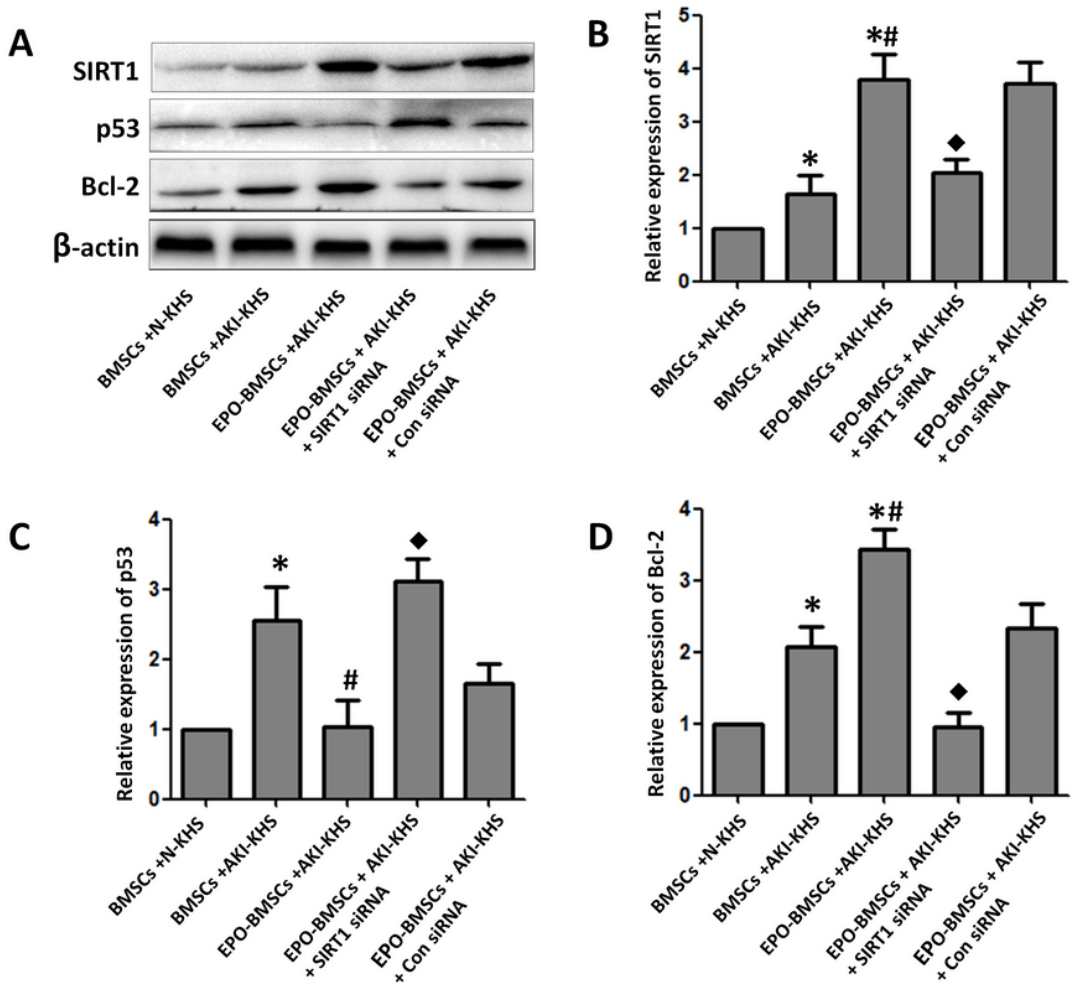

Figure 3

Protein expression pattern of each group. (A) Western blot analysis of the anti-apoptotic factor Bcl-2, the pro-apoptotic factor p53, and SIRT1. (B) Relative expression of SIRT1. (C) Relative expression of p53. (D) Relative expression of Bcl-2. *p < 0.05 versus BMSCs+N-KHS, #p < 0.05 versus BMSCs+AKI-KHS, ◆p< 0.05 versus EPO-BMSCs+AKI-KHS.

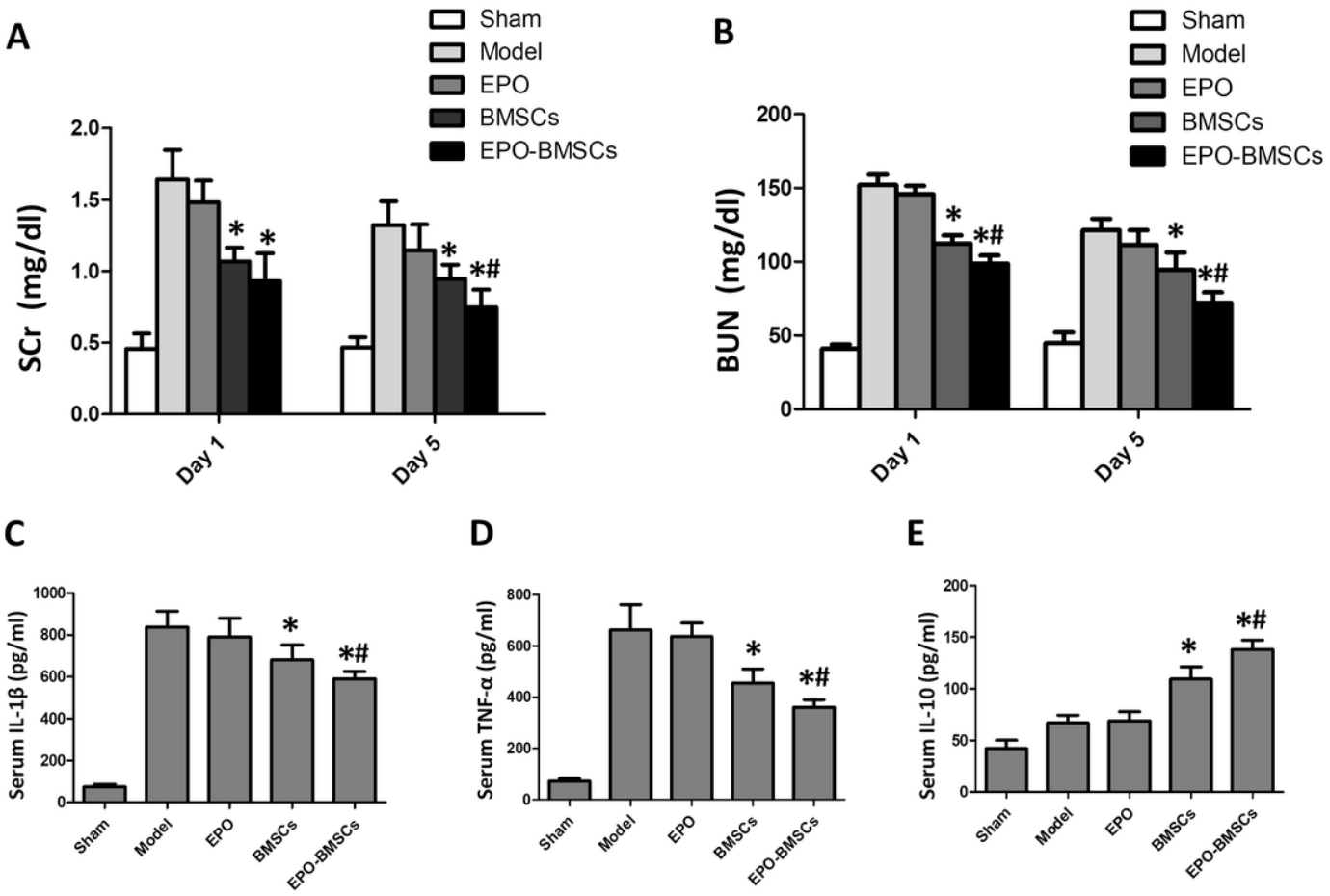

Figure 4

The effect of BMSC and EPO-BMSC treatment on AKI rats. Serum level of (A) SCr and (B) BUN measured on day 1 and 5 after treatment. Serum level of the pro-inflammatory cytokines (C) IL-1β and (D) TNF-α and the anti-inflammatory cytokine (E) IL-10 measured by ELISA 24 h after the indicated treatment.*p < 0.05 versus Model group, #p < 0.05 versus BMSCs group.

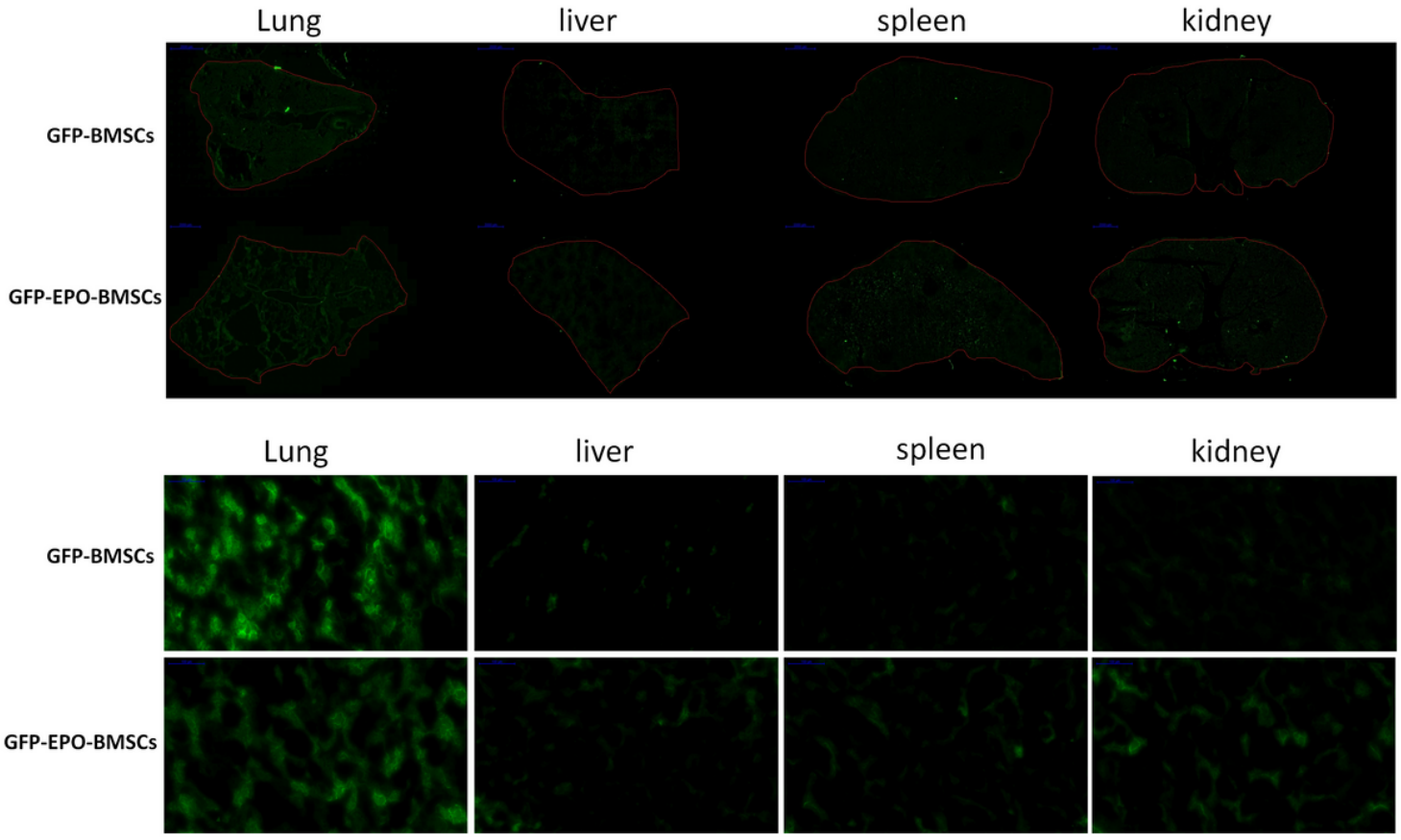

Figure 5

GFP fluorescence images of frozen sections from the lung, liver, spleen, and kidney of rats. Sections were prepared 24 h after intravenous infusion of BMSCs and EPO-BMSCs.

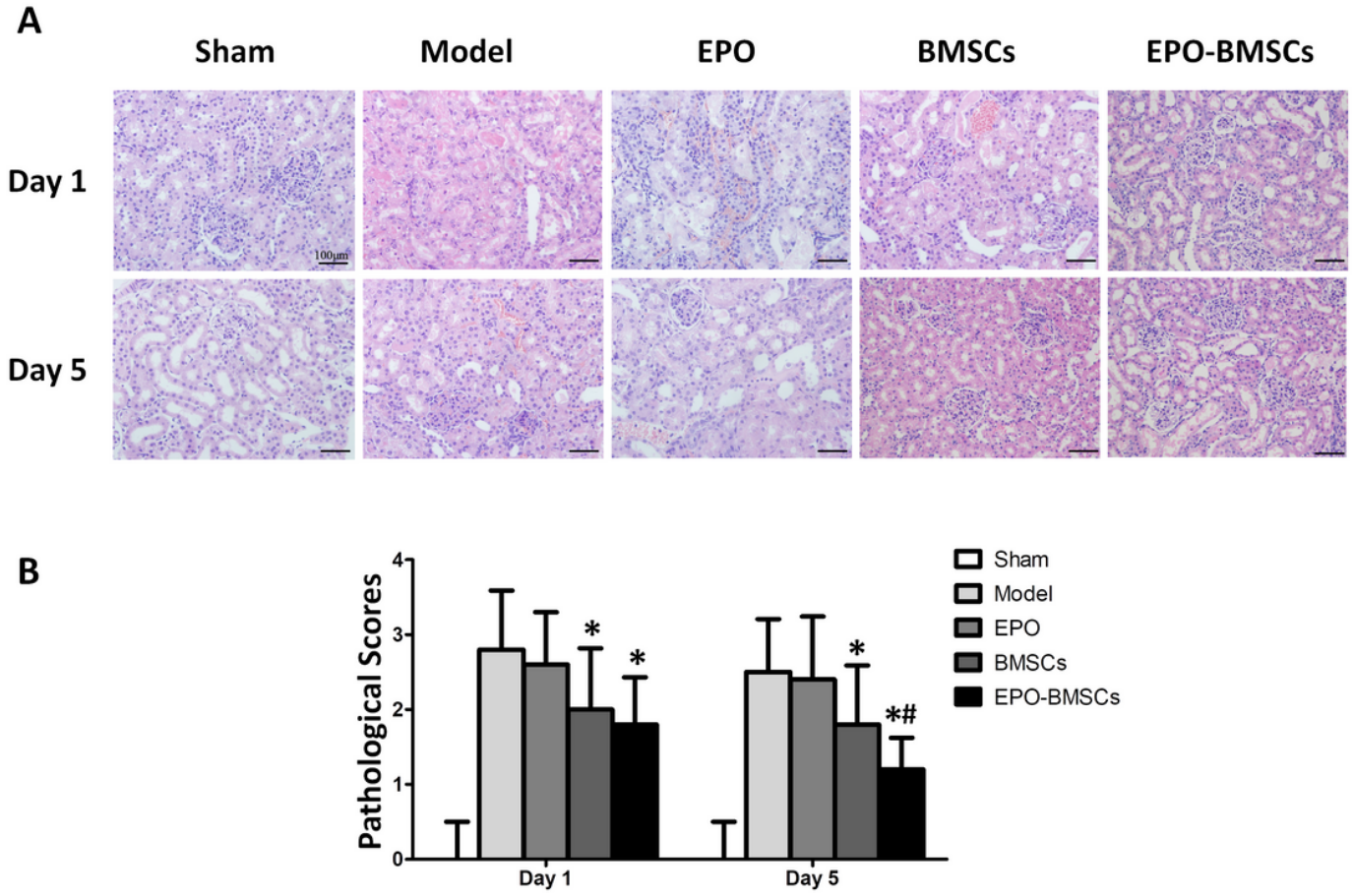

Figure 6

Histological analysis. (A) Kidney sections stained with HE on day 1 and 5 after each treatment. (B) Pathological score of each group one and five days after each treatment.*p < 0.05 versus model group; #p < 0.05 versus BMSCs group.